

Article

An H5 Transformerless Inverter for Grid Connected PV Systems with Improved Utilization Factor and a Simple Maximum Power Point Algorithm

Hani Albalawi ¹ and **Sherif Ahmed Zaid** ^{2,*}

¹ Department of Electrical Engineering, Faculty of Engineering, University of Tabuk, Tabuk 47913, Saudi Arabia; halbala@ut.edu.sa

² Department of Electrical Power, Faculty of Engineering, Cairo University, Cairo 12613, Egypt

* Correspondence: shfaraj@ut.edu.sa or sherifzaid3@yahoo.com

Received: 19 October 2018; Accepted: 23 October 2018; Published: 25 October 2018



Abstract: Due to their small size, minimum cost, and great efficiency, photovoltaic (PV) grid-connected transformerless inverters have been developed and become famous around the world in distributed PV generators systems. One of the most efficient topologies of the transformerless inverter family is H5 topology. This inverter extracts a discontinuous current from the PV panel, which conflicts with the operation at maximum power point tracking (MPPT) conditions while the utilization factor of the PV degrades. This paper proposes improved H5 topology featuring a boost converter inserted in the middle between the PV panels and the H5 inverter. The design of the boost converter is planned to operate at continuous conduction mode to guarantee MPPT conditions of the PV. A new and simple off line MPPT algorithm is introduced and performance factors like efficiency and utilization factors of the proposed and convention H5 topology are compared. The simulation results indicate that the proposed system provides a preferable utilization factor and a simpler MPPT algorithm.

Keywords: PV panel; H5 inverter; boost converter; MPPT; utility grid; utilization factor

1. Introduction

Among all renewable energy sources, photovoltaic (PV) energy is generally rated as the most attractive and sustained source because it is available throughout the year. In the future, more than 45% of the needed power is anticipated to be generated by PV arrays. The cost of these systems depends on the PV module size. Therefore, to reduce the cost of a PV system, the electric power driven by the PV must be efficiently consumed. Altered system structures can be used to enhance overall system efficiency [1–3].

PV arrays can deliver energy to stand-alone applications or utility grids. Delivering power to a utility grid is becoming an increasingly popular option [4–8]. To connect PV arrays to the utility grid, the DC/AC inverter followed by a line transformer is used [9]. The line transformer realizes the following goals: (1) galvanic separation between the PV array and the utility electricity network and consequently achieves individual protection and safety, and (2) raises the voltage produced by the inverter to a suitable value to meet the utility grid voltage. These transformers have many drawbacks including high system cost and decreased efficiency. The transformers are very large and heavy. Without a line transformer, leakage current forms through parasitic capacitances between the PV array and the ground [10–12]. The leakage current results in radiated interfering problems and other severe safety issues; the current must be reduced to limited values [10]. The German DIN VDE 0126-1-1 standard [13] restricts the values of the leakage current in a PV grid-connected system.

The leakage current is produced due to the alternation in the common mode (CM) voltage of the inverter. The variation of the CM voltage must be minimized to diminish the leakage current.

To resolve the issue concerning leakage current, several solutions can be used. Conventional half-bridge inverters can be utilized, but the main problem involves dc voltage utilization at 50% and the significant number of PV arrays needed [14]. Conventional full-bridge inverters with bipolar or unipolar SPWM can solve the problems created by half-bridge inverters [15]. With bipolar SPWM, the current ripples in the filter inductors and switching losses are high while with unipolar SPWM the common mode voltage changes at switching frequency, something which results in high leakage current. Another approach to minimize leakage current is to employ transformerless inverters [16–19]. The basic idea of transformerless inverters is to disconnect the dc side (PV array) from the ac side (inverter and grid) in freewheeling modes. Consequently, the CM voltage is kept nearly constant. Transformerless PV systems demonstrate the advantages of lower cost, lower system size, and higher efficiency when compared to line transformer systems. Several topologies have been developed in the literature including highly efficient and reliable inverter concept (HERIC) topology, such as H5 and H6 topologies. Various versions with modifications to those transformer-less inverters have been introduced [20–22]. Each topology has its own benefits and drawbacks involving the ability to reduce leakage current, the number of switches and their total losses, and system efficiency and cost. Among these inverters, an H5 inverter has been chosen as a case of study. These inverters have the fewest number of switches (5 switches) which leads to a reduced cost and a simpler overall inverter compared to other inverters. Therefore, H5 topology has been adopted by SMA Solar Technology AG [23], the world's biggest producer of inverters. The only problem is the high conduction losses where three switches conduct together during active modes.

Several studies have been reported in the literature regarding H5 inverter. Reference [24], reports a serious CM current in practical applications due to its asymmetric structure. The authors propose an electromagnetic interference (EMI) filter to suppress the CM current, but the EMI filter will increase the size and weight as well as the cost of the inverter. An effective H5 topology [25] called H5-D topology, is introduced to suppress CM current in the inverter with H5 topology. However, the main weakness of that topology is its complexity.

When employing transformer-less systems, researchers have considered the maximum power drawn from the PV system. Hence, it is important to follow up the maximum power to improve the utilization factor of the PV system. A maximum power point tracker is also used to continuously draw maximum power from the PV array. Many MPPT techniques have been developed and are part of the literature [26–30]. There are two ways to track the maximum power point (MPP) of a PV panel, electrical and mechanical tracking. Electrical tracking depends on the P-V and I-V curves of a PV panel, while mechanical tracking is based on changing the PV panel orientation according to the Sun's position. In practice, fixed PV panels are preferred due to their higher robustness and lower cost. Usually, electrical MPPT tracking techniques are employed. The MPPT can be categorized into offline, online, and hybrid method. Some of the MPPT online techniques include the Perturb and Observe (P&O) method, Incremental Conductance (IC) method, Artificial Neural Network method, and Fuzzy Logic method [31–35]. The online techniques are precise and compensate for different disturbances. However, it is more complex and needs higher cost than offline techniques. Offline techniques are considered the easiest to apply using several algorithms in the literature [28]. The Fractional Open Circuit Voltage (FOCV) and Fractional Short Circuit Current (FCCC) are common methods of the offline techniques. Using the FCCC method enhances the system efficiency than FOCV [30]. Unfortunately, the H5 inverter structure with the conventional operation has a general problem. Which is the H5 structure is disconnected the PV panel from the utility grid during zero state mode. Therefore, the PV panel utilization factor (K_u) drops to small fractional values, where this factor should be near unity to improve the cost and the size of the PV panel [36].

This paper proposes an improved H5 topology to increase the PV panel utilization factor and extract maximum power from the PV panel. The proposed system featuring a boost converter inserted

between the PV panel and the H5 inverter. The boost converter is used as an impedance matching device between the PV array on one side and the H5 inverter and the grid on the other side. It is designed to operate at continuous conduction mode, such that the PV current is continuous at the MPPT value. The maximum power point tracker is a simple offline technique uses the FCCC method. However, the FCCC is modified using curve-fitting techniques to generate the duty cycle that drives the boost converter with the PV at MPPT. On the other hand, the utilization factor of the system is improved by extracting continuous current from the PV. A theoretical explanation for the system utilization factor improvement is presented. Also, the reduction of leakage current to reasonable values according to commonly accepted standards is achieved. The performance factors like efficiency and utilization factors of the proposed and convention H5 topology are compared. The simulation results indicate that the proposed system provides a preferable utilization factor and a simpler MPPT algorithm.

This paper is arranged as follows: Section 2 includes discussion of the conventional H5 converter operation and utilization factor analysis and calculations. Section 3 presents the proposed improved H5 inverter system. All controllers of the improved H5 and control approaches are found in Section 4. Simulation results and their discussions are presented in Section 5. Finally, Section 6 shows the conclusions.

2. Conventional H5 Converter

Figure 1 shows the conventional H5 transformerless inverter topology. In the figure, the conventional H-bridge inverter is connected to the PV panel using the fifth switch. The switch operates at the same frequency as the utility grid's frequency. Moreover, it works to disconnect the PV array from the grid in zero state, something which cuts off the path for leakage current. As a result, system leakage current is greatly decreased. The H5 topology has fewer power switches than other topologies like HERIC and H6.

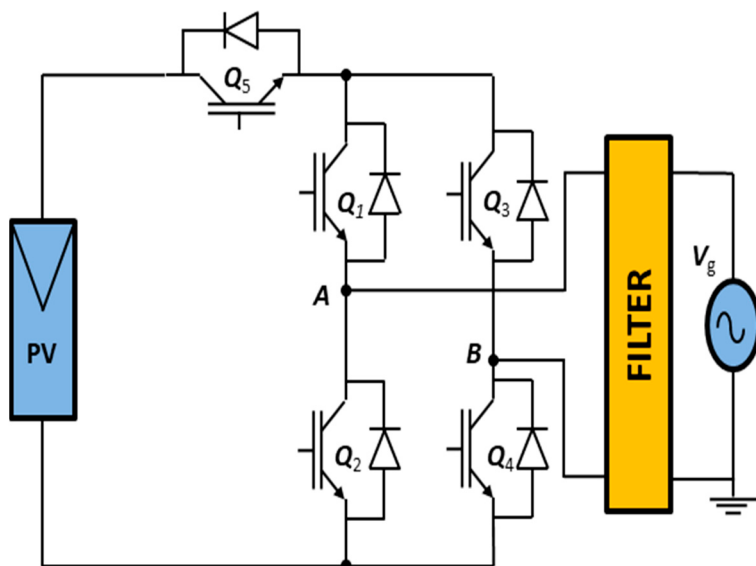


Figure 1. H5 inverter topology.

2.1. Conventional H5 Converter Operation and Control

The following main operation principles for the H5 inverter are summarized in Figure 2:

- The upper group switches (Q1 and Q3) operate alternately at the grid frequency. (Q1) is on during the positive half cycle, while (Q3) is on during the negative half cycle. The control signals of switches (Q1 and Q3) are pure square waves at the supply frequency.
- The lower group switches (Q2 and Q4) operate alternately at the grid frequency. (Q4) is on during the positive half cycle, while (Q2) is on during the negative half cycle. The control signals of

- switches (Q2 and Q4) are square waves at the supply frequency, but are modulated with PWM as shown in Figure 2.
- The switch (Q5) operates with PWM simultaneously with either switch (Q4) in the positive half cycle or switch (Q2) in the negative half cycle.

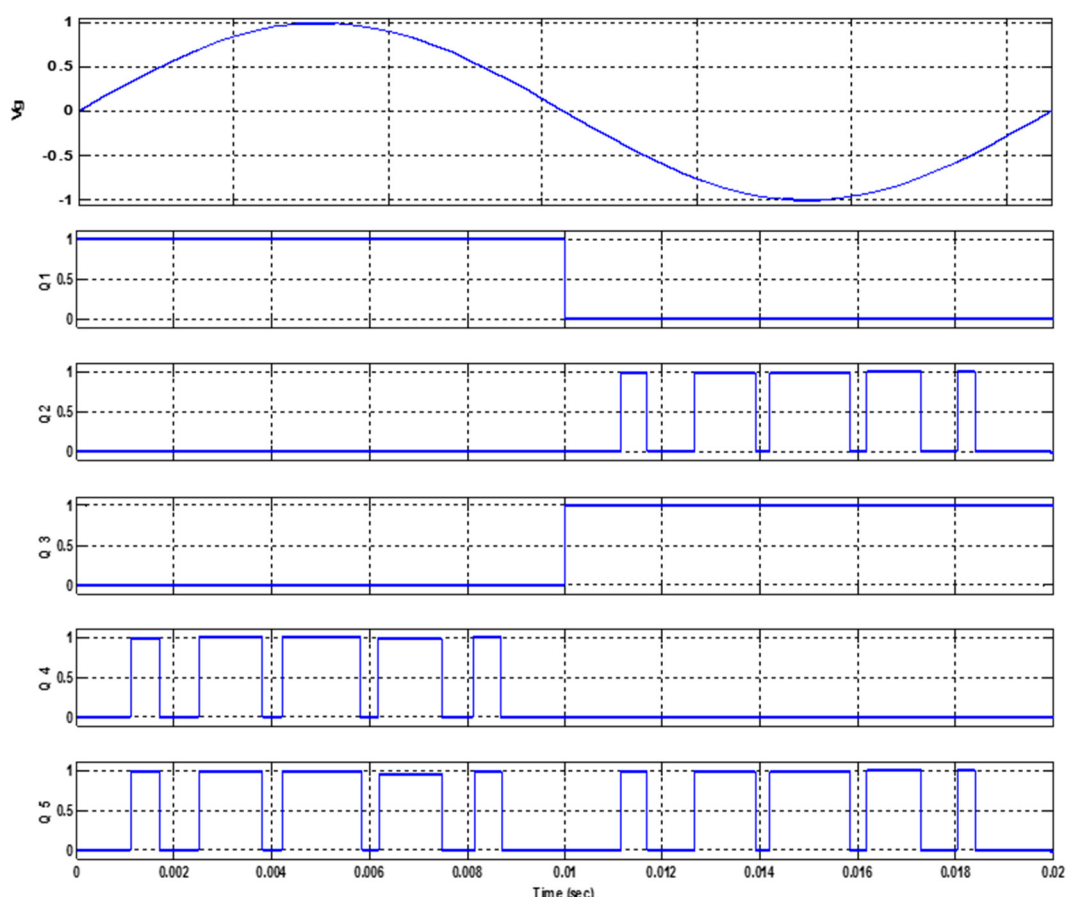


Figure 2. Control signals of H5 inverter switches.

The operation of the H5 inverter may be divided to four modes. The first mode is named the active state mode and the current passes via Q_5 , Q_1 , and Q_4 from the PV panel to the grid as presented in Figure 3a. The second mode is named zero state mode since there is no energy transfer from the PV to the grid. In this mode, the grid current freewheels through Q_1 and D_3 , but the PV panel is disconnected from the grid as shown in Figure 3b. Figure 3c demonstrates the route of the third mode, it is also an active state mode. In which, the current circulates over Q_5 , Q_3 , and Q_2 from the PV unit to the grid. The fourth mode is also called the zero state mode. In this mode, the grid current freewheels via Q_3 and D_1 , and the PV panel is disconnected from the grid as shown in Figure 3d.

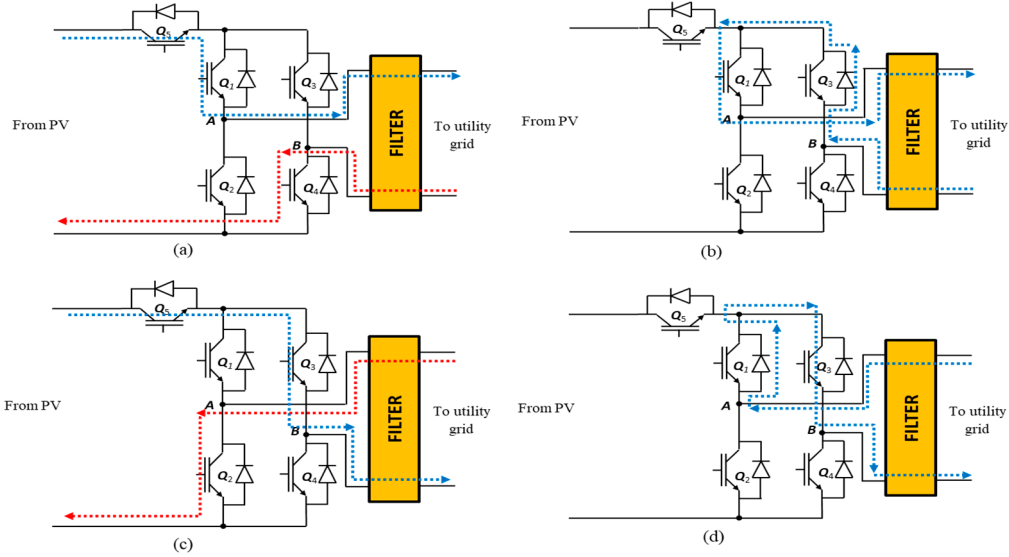


Figure 3. H5 inverter modes of operation (a) mode 1, (b) mode 2, (c) mode 3 and (d) mode 4.

The conventional H5 inverter has three controllers; namely, the grid current controller, the DC link voltage controller, and the MPPT controller. The first two controllers are typically the same as the proposed counterparts that will be discussed with the proposed system. However, the third controller, the MPPT controller, function is to extract maximum power from the PV. This control loop has a very slow response compared to the first two controllers, due to the fact that insolation fluctuations are usually slow. As mentioned before, there are many MPPT techniques in the literature, but, the incremental conductance method is selected for the conventional system. The details of the incremental conductance method are presented in [37].

2.2. Utilization Factor of a PV Array Supplies Conventional H5 Inverter

The utilization factor, K_u , is a factor that measures how the PV utilizes the solar incident power. It is defined as the average generated power from the PV (P_{PV}) divided by the maximum power that can be generated P_{MPPT} and is given by [37,38]:

$$K_u = \frac{P_{PV}}{P_{MPPT}} \quad (1)$$

P_{PV} and P_{MPPT} are approximately calculated to determine K_u . Knowing the typical currents supplied by the PV array to the H5 inverter as shown in Figure 4, the average generated PV power (P_{PV}) at a certain operating point is given by:

$$P_{PV} = 2f_g \int_0^{0.5/f_g} v_{pv} i_{pv} dt \quad (2)$$

where v_{pv} is the PV voltage, i_{pv} is PV current, and f_g is the grid frequency.

At maximum power point condition and for simplicity, $v_{pv} = V_{MPPT}$, which is a constant value. Therefore, the average output power of the PV array is:

$$P_{PV} = 2f_g V_{MPPT} \int_0^{0.5/f_g} i_{pv} dt \quad (3)$$

Due to the discrete nature of i_{pv} as shown in Figure 4, the integration sign is replaced by a summation:

$$P_{PV} = 2f_g V_{MPPT} \sum_{j=1}^{0.5m_f} \delta_j i_{pv}(j) \quad (4)$$

where δ_j is the pulse width, j is the pulse order, m_f is the modulation frequency ratio, and m is the modulation index. Knowing the values of δ_j and $i_{pv}(j)$ for each pulse [37], Equation (4) becomes:

$$P_{PV} = \frac{m}{0.5m_f} I_{MPPT} V_{MPPT} \sum_{j=1}^{0.5m_f} \sin^2\left(\frac{j\pi}{0.5m_f}\right) \quad (5)$$

By substituting Equation (5) into Equation (1) with the help of trigonometric relations, the result is:

$$K_u = 0.5m \left[1 - \frac{1}{m_f} \sum_{j=1}^{0.5m_f} \cos\left(\frac{j\pi}{0.25m_f}\right) \right] \quad (6)$$

Generally, for unipolar SPWM m_f should be an even integer. Therefore, the summation part in Equation (6) will be zero. Therefore:

$$K_u = 0.5 m \quad (7)$$

Hence, for a PV-H5 inverter conventional system, the MPPT condition is not precise and the factor K_u is lower. These changes occur as a result of the non-continuous PV current as shown in Figure 4.

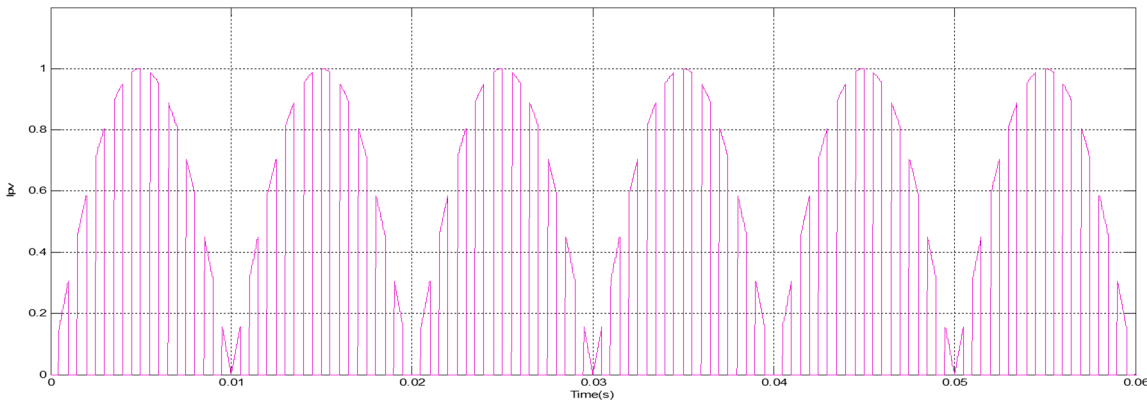


Figure 4. H5 inverter typical.

3. Proposed H5 Converter System

From the previous analyses of the classical H5 inverter connected to a PV system, the utilization factor K_u is low, and may be equal to 0.5. The MPPT conditions of the PV could not be attained. The source of the problem is the discontinuous current from the PV panel. The boost converter has the ability to deliver continuous input current. The cause of the problems can be eliminated by attaching a boost converter to the system as presented in Figure 5. The boost converter input current value is adapted to provide the proper MPPT conditions for the PV panel.

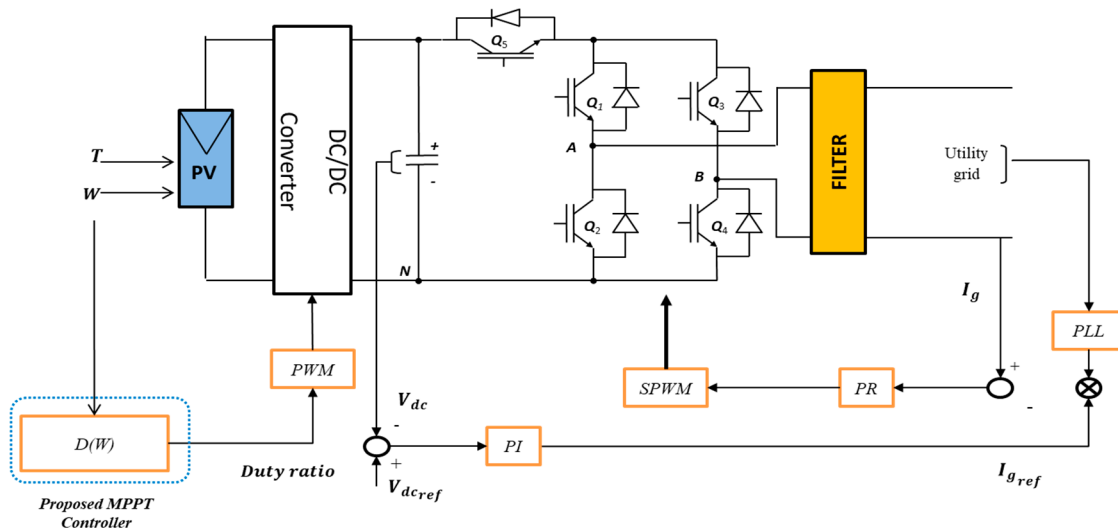


Figure 5. Proposed system with controllers.

4. Proposed System Controllers

The control system of the proposed PV-grid connected system is divided into two phases. The first control phase is the MPPT controller. This step extracts maximum power from the PV panel. Based on the insolation level, PWM pulses are generated for the boost converter. The duty cycle derives the PV panel into the MPPT conditions. The second phase is the H5 controller. The controlled parameters of this stage involve the DC link voltage and grid current. Figure 5 shows the two nested loops of the stage. The inner loop is the grid current regulation loop and the outer loop is the DC link voltage regulation loop.

4.1. MPPT Controller

The installation of PV systems has grown due to the increasing demand for energy and environmental awareness. The variability of solar irradiation has created challenges in extracting maximum power. Hence, many techniques have been prepared for MPPT [26,27]. The MPPT can be categorized into offline, online, and hybrid method. This paper focuses on the offline method which uses a reference signal like a short circuit current, open circuit voltage, solar irradiation, and temperature to generate the control signal to track MPP [27].

The Fractional Open Circuit Voltage (FOCV) and Fractional Short Circuit Current (FCCC) are common methods of the offline techniques as they isolate the PV array and determine the operation point for the MPPT. These techniques are easy to implement, but result in periodic power loss due to the periodic isolation of the PV array. The FCCC is based on approximating the current at MPP to be equal to the short circuit current by factor k ($I_{mpp} \cong kI_{sc}$) where k varies between 0.71 and 0.90 based on the PV array datasheet [28,29]. The main issue of FCCC is the difficulty associated with measuring the short circuit current when the PV system is operating [29]. The FOCV is based on the fact that the voltage of the PV array at MPP is approximately linearly proportional to the open circuit voltage by a factor of k ($V_{mpp} \cong kV_{oc}$) where k varies between 0.71 and 0.80 based on the PV array datasheet [30].

One of the offline techniques uses curve fitting based MPPT which uses panel characteristics curves to find a mathematical model for MPPT. The MPPT in this paper is based on the P-V characteristic curve. The data sheet for the PV panel is used to generate the P-V curves for different irradiation points as shown in Figure 6.

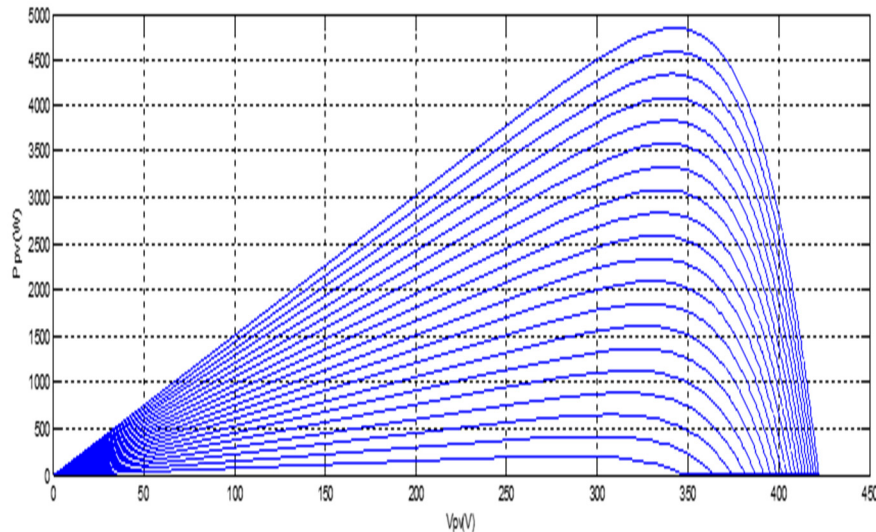


Figure 6. P-V characteristics curves.

Proposed MPPT Controller

The input for this controller is the insolation level (W), while the output is the boost converter duty value, $d(t)$, shown in Figure 5. The boost converter output is regulated to be constant at V_{DC} ($V_{DC} = 450$ V) by the H5 converter controller. Assuming continuous conduction of the boost converter, the input-output voltage relation is given in the following equation:

$$\frac{V_{DC}}{V_{pv}} = \frac{1}{1 - d(t)} \quad (8)$$

To operate the PV system at the MPPT conditions, its terminal voltage must be equal to V_{mpp} , the voltage at MPP. The duty cycle at MPPT conditions (d_{mpp}) as determined by the following equation:

$$d_{mpp} = 1 - \frac{V_{mpp}}{V_{DC}} \quad (9)$$

The voltage value of V_{mpp} is determined by using the PV characteristic curves for each insolation level as shown in Figure 6. A table relating the duty cycle, d_{mpp} , to the insolation level is calculated as shown in Table 1.

Table 1. Duty cycle ratio at MPPT conditions (d_{mpp}) corresponding to each Irradiation (W, @ 25 °C).

W	50	100	150	200	250	300	350	400	450	500	750	1000
d_{mpp}	0.351	0.328	0.318	0.304	0.296	0.287	0.278	0.273	0.267	0.262	0.247	0.239

To simplify the system and controller, the values provided in Table 1 are converted to a function. The function uses curve-fitting techniques and the duty cycle that provides d_{mpp} as a function of W can be determined by:

$$d_{mpp}(W) = 2.266e^{-13}W^4 - 6.478e^{-10}W^3 + 7.405e^{-7}W^2 - 0.0004498W + 0.3698 \quad (10)$$

The MPPT control loop is commonly much slower than the H5 converter controller, as the insolation changes are very slow. Referring to Figure 5, the temperature is an input signal to the controller. The data of table [1] is given at 25 °C. For different temperatures, the data of table [1] differs for any given temperature. However, in this paper the temperature that used for simulation is 25 °C.

4.2. H5 Converter Controller

This controller has two objectives. The first objective is to maintain the voltage, V_{DC} , at a constant value. The second objective involves forcing the grid current tracking to a certain reference value. The controller has two nested loops; the inner loop is for the grid current and the outer loop is for the V_{DC} . Generally, the inner control loop needed to be quicker than the outer loop for stable operation [39–42].

- *Outer Loop:* The large capacitor value at the H5 converter input slows the speed of response. A simple PI controller is adapted for this loop. The proportion and integral gains, the PI controller, are tuned using Niche hols-Ziegler method.
- *Inner Loop:* The reference signal for this loop is a sinusoidal wave with a grid current reference. The magnitude of the wave comes from the outer loop controller and the phase comes from the PLL synchronized to the utility grid. The Proportional Resonant (PR) controller is often used for grid-connected inverters [43,44]. This type of controller is very useful with sinusoidal reference signals which provide a more acceptable response than PI controllers. The PR controller transfer function, $PR(s)$, is:

$$PR(s) = k_p + \frac{k_i s}{s^2 + \omega_0^2} \quad (11)$$

where, k_p and k_i are the proportional and resonant gains respectively; ω_0 is the resonant angular frequency. The tunings of the controller parameters are based the techniques in reference [44].

5. Simulation Results

The conventional and proposed transformerless H5 inverter systems attached to the PV array shown in Figures 1 and 5 are simulated using the Matlab/Simulink software package. The system parameters are listed in Table 2. The PV array for the conventional and proposed systems has the same total number of PV modules, but the number of parallel and series PV modules are different to provide the same DC bus voltage, V_{DC} . The PV panel structure for the conventional version is 960 series cells \times 3 parallel strings, while the proposed is 720 series cells \times 4 parallel strings. The total number of cells for the two arrangements is the same (2880 cell). The boost converter switching frequency was 10 KHz.

Table 2. System Parameters.

System	Parameter	Value
Proposed	PV SC current	11.7 A
	PV OC voltage	562 V
	PV SC current	16.35 A
	PV OC voltage	422 V
	C_f	2 nF
	L_f	1.8 mH
Proposed	Utility voltage	230 V
	Utility frequency	50 Hz
	PWM carrier frequency	10 KHz
	DC link capacitor	2000 μ F

The waveforms of the grid voltage, grid current, PV current, and leakage current for the conventional and proposed systems are shown in Figure 7. In both systems, the grid current is controlled to ensure it is in phase with the grid voltage to ensure a unity power factor operation. Also, the earth leakage currents have nearly the same RMS current (18 mA), which is within the standard recommended values [45]. In the proposed system, the PV current is constant and equal to the maximum power point current. This set up emphasizes MPPT operation of the proposed system. The PV current for the convention system is discontinuous, indicating a low Ku value and the MPPT condition does not work.

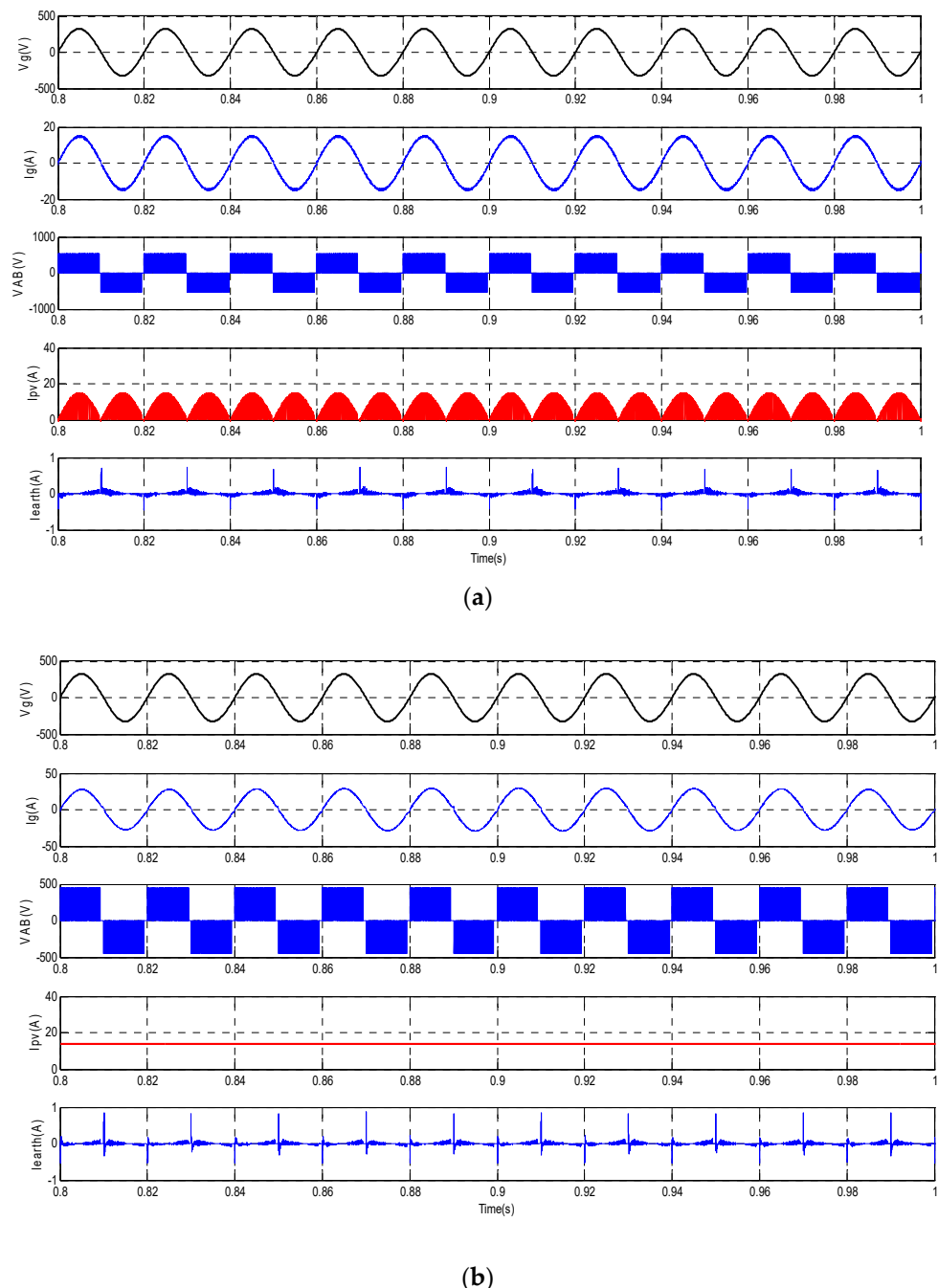


Figure 7. Simulation result of inverter voltage, grid current, PV current, and earth leakage current of the (a) conventional H5 inverter and (b) H5 proposed inverter.

Figure 8 shows the utilization factor variations of various output power levels for both the proposed and conventional systems. Figure 8 shows that the K_u of the conventional H5 is as low as 50%, which is the value predicted by previous analyses. The proposed system has a K_u of 100%, which is a natural result for the true MPPT operation. If a coupling capacitor (2000 uF) is added at the input of the conventional H5 converter, the PV K_u is improved as shown in Figure 8. However, the proposed system K_u still better than the conventional though with the coupling capacitor addition. It is noticed that, for operating powers less than 50% of the rated power, the effect of the coupling capacitor is weak and K_u is low. On other hand, for operating powers greater than 50% of the rated power, the K_u is near 100%. Also from simulations, it is found that the efficiency of the conventional system have not been significantly affected by coupling capacitor insertion. The Californian utilization factor $|k_u|_{CE}$ is calculated by the following equation:

$$k_u|_{CE} = 0.53k_u|_{75\%} + 0.04k_u|_{10\%} + 0.05k_u|_{20\%} + 0.12k_u|_{30\%} + 0.21k_u|_{50\%} + 0.05k_u|_{100\%} \quad (12)$$

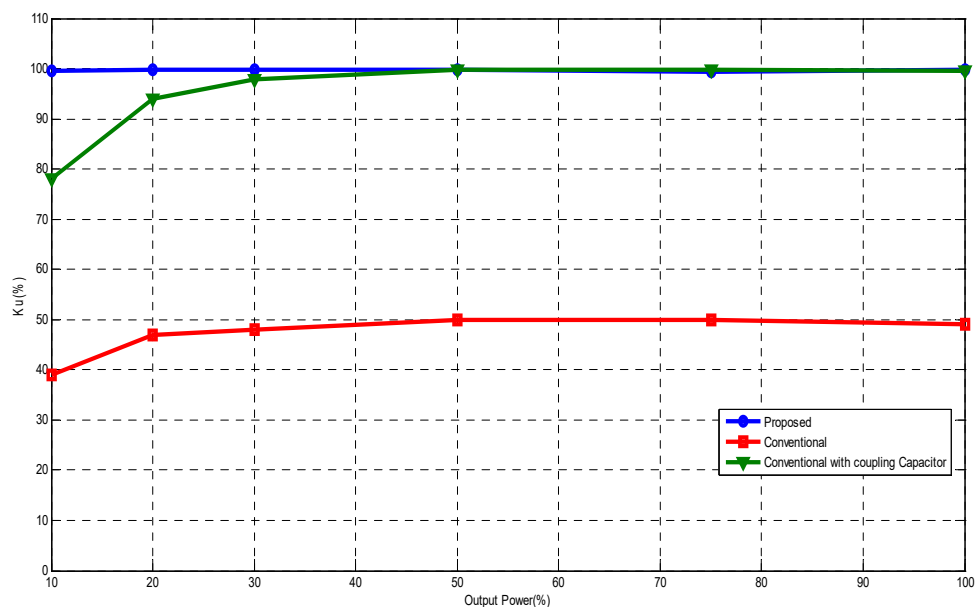


Figure 8. The variations of K_u with output power of both conventional and proposed systems.

The Californian utilization factors for the conventional, conventional with coupling capacitor, and proposed H5 approaches were calculated by using Equation (12) to be 56%, 98.4%, and 99.9%, respectively.

Figure 9 demonstrates the efficiency variations at various output power levels for both the proposed and conventional systems. It is noticed that the efficiency in both approaches were close. The proposed system has slightly lower efficiency than the conventional system due to the added boost converter losses. The efficiency has a peak value of nearly half the nominal output power.

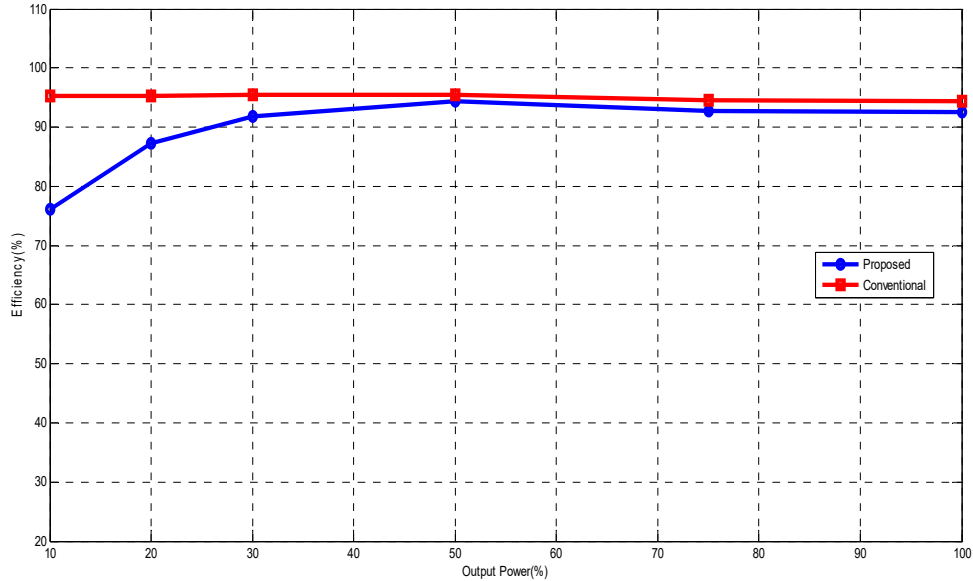


Figure 9. The variation of system efficiency with output power of both conventional and proposed systems.

The Californian efficiencies for the conventional and proposed H5 approaches were calculated using Equation (13) to be 95% and 93%, respectively:

$$\eta_{CE} = 0.53\eta_{75\%} + 0.04\eta_{10\%} + 0.05\eta_{20\%} + 0.12\eta_{30\%} + 0.21\eta_{50\%} + 0.05\eta_{100\%} \quad (13)$$

Figure 10 both proposed and conventional transformerless H5 inverter system. The THD of the proposed system is usually smaller than the THD of the traditional system. The proposed systems provide high quality, clean power to the utility grid. At low power levels ($\leq 20\%$), the THD increases slightly. The slight increase does not create an issue if the injected power is low.

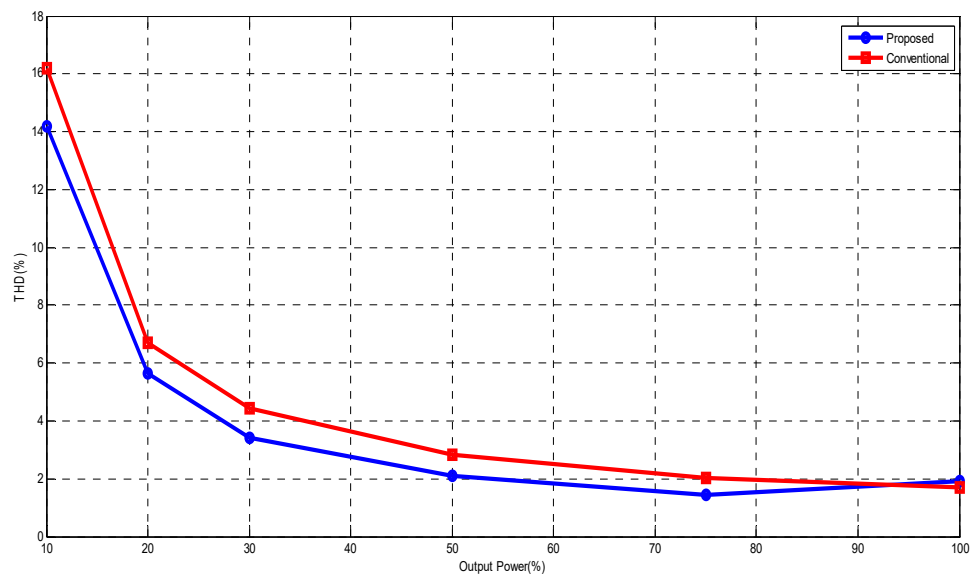


Figure 10. The variations of THD with output power of the conventional and proposed systems.

The harmonic spectrums of the grid currents for both systems are shown in Figure 11. The order harmonics appear in both spectrums and the i_g harmonics in the spectrum of the proposed system are fairly smaller than the harmonics present in a convention system. Generally, the THD of the proposed system is smaller than that in the traditional system.

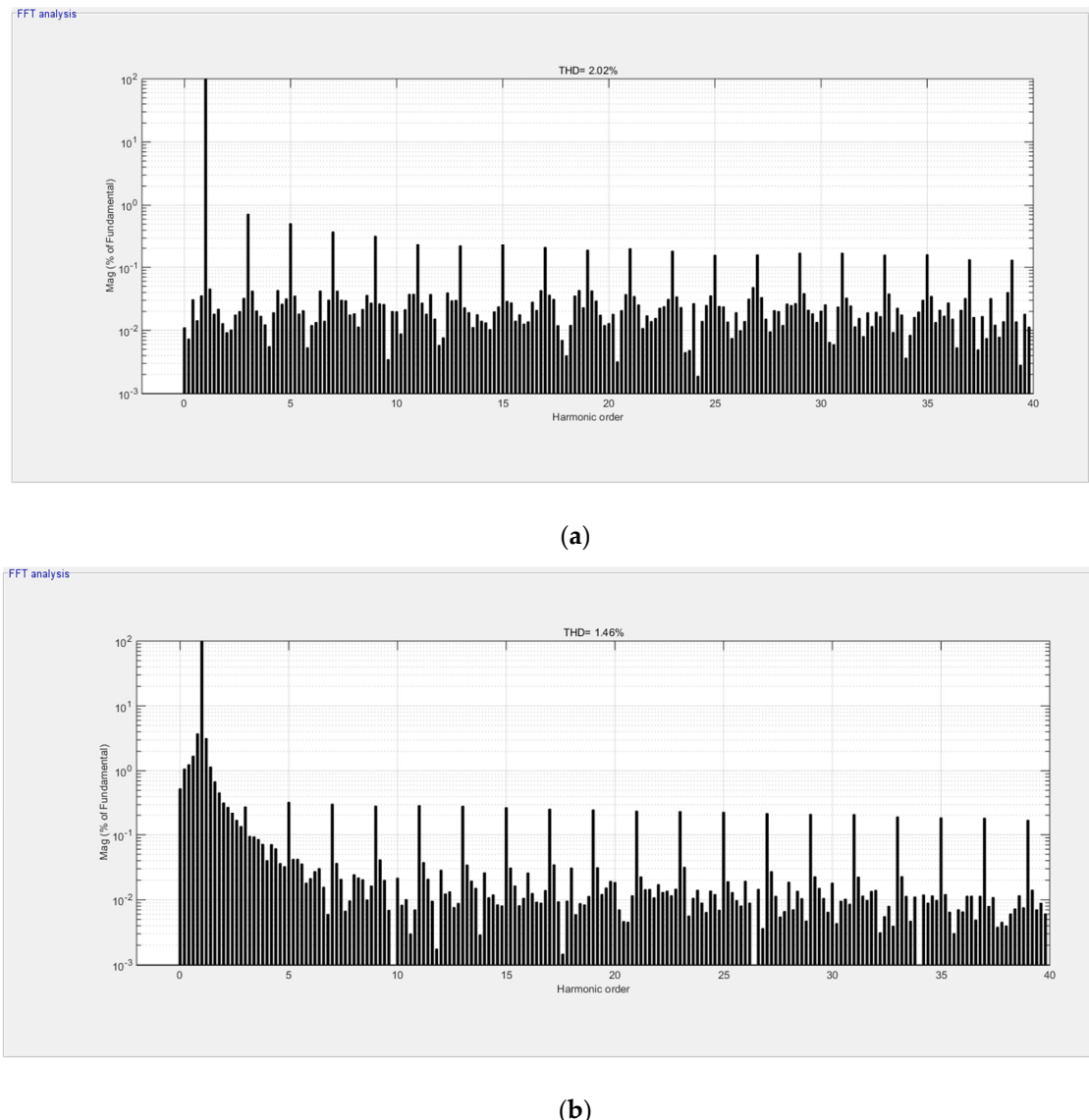


Figure 11. The harmonic spectrum of the (a) conventional and (b) proposed at 75% insolation.

The proposed MPPT algorithm is compared to the traditional MPPT with the Incremental Conductance (IC) method. Figure 12 shows the MPPT power, output power, and boost converter duty ratio (d) responses for the proposed system at step insolation changes. It is seen that the output power tracks the MPPT power with a small steady state error that represents circuit losses. A relatively slow power response is also noticed due to the large capacitors of the system and the open-loop MPPT control technique used. The duty ratio (d) generated by the controller changes in a way that forces the boost converter and PV to operate at MPPT conditions. The duty ratio changes in a narrow range ($20\% < d < 34\%$), for insolation variations ($10\% < I < 100\%$). Figure 13 illustrates the MPP power, output power, and boost converter duty ratio (d) responses for the conventional MPPT control system at step insolation changes. The output power responses in Figures 12 and 13 are similar; however, the proposed controller is very simple.

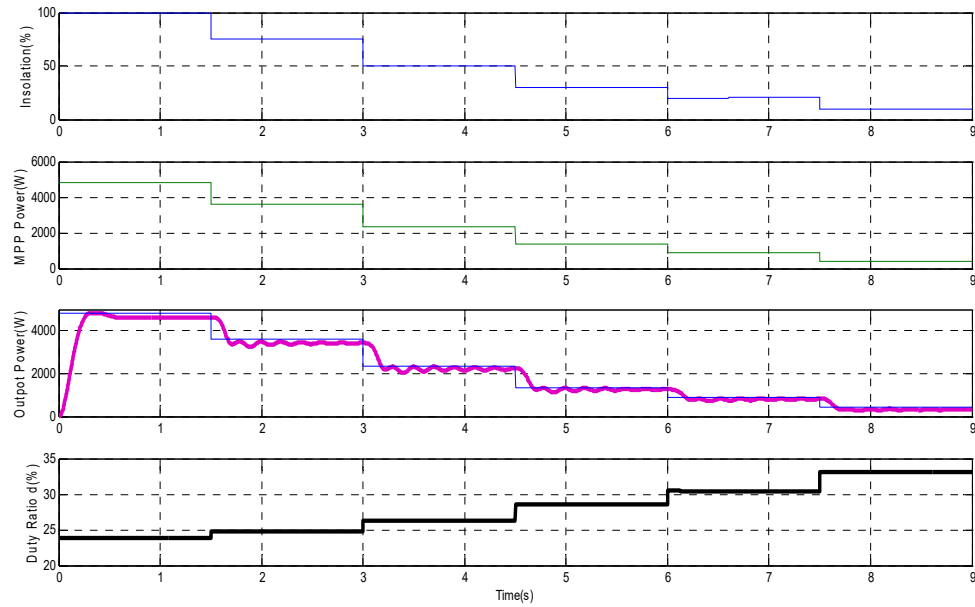


Figure 12. The MPP power, output power, and boost converter duty ratio (d) for the proposed system at step insolation changes.

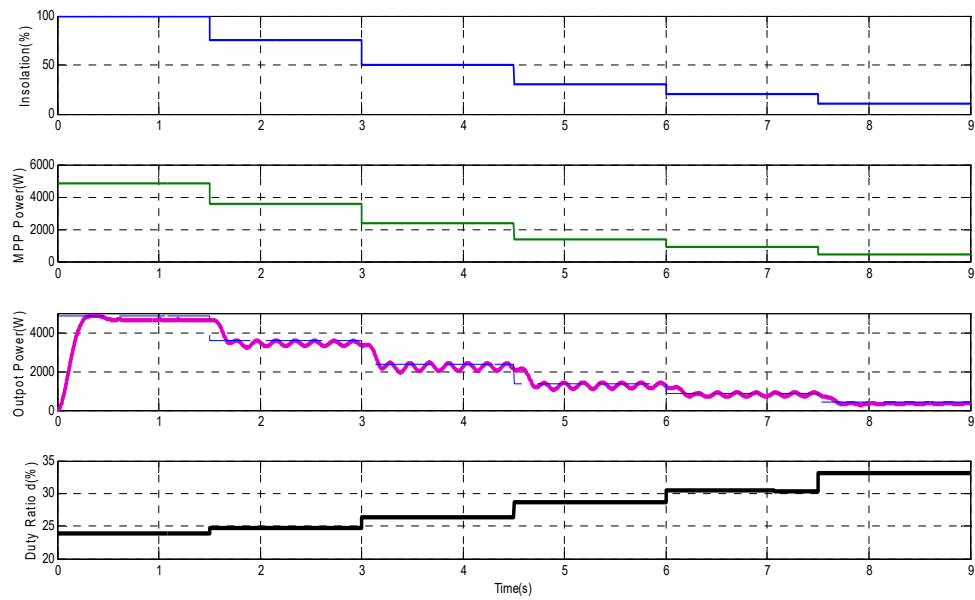


Figure 13. The MPP power, output power, and boost converter duty ratio (d) for the conventional MPPT system at step insolation changes.

6. Conclusions

This paper proposes an improved topology for the H5 transformerless inverter supplied by a PV panel. The proposed topology improves some performance factors like the utilization factor and maximum power point operation. In addition, a simple off-line MPPT algorithm is introduced. Simulation results show that the proposed system has a better utilization factor (nearly 100%) than the conventional system. The proposed system has a small drop in efficiency compared to the drop seen in the conventional system. The paper also compares the operation of the PV in the proposed system to the traditional system with MPPT conditions. The comparison has found that the proposed MPPT algorithm is simpler than the traditional system.

Author Contributions: S.Z. conceived and designed the system model. S.Z. and H.A. analyzed the data and results. H.A. wrote the paper.

Funding: This research was funded by UNIVERSITY OF TABUK, grant number S-1439-0058 at <https://www.ut.edu.sa/web/deanship-of-scientific-research/home>.

Acknowledgments: The author would like to acknowledge the Deanship of Scientific Research of University of Tabuk for its great support.

Conflicts of Interest: The authors declare no conflict of interest.

References

1. Calais, M.; Myrzik, J.; Spooner, T.; Agelidis, V.G. Inverters for single-phase grid connected photovoltaic systems—an overview. In Proceedings of the 2002 IEEE 33rd Annual Power Electronics Specialists Conference, Cairns, Australia, 23–27 June 2002; pp. 1995–2000.
2. Suan, F.T.K.; Rahim, N.A.; Hew, W.P. Modeling, analysis and control of various types of transformerless grid connected PV inverters. In Proceedings of the 2011 IEEE First Conference on Clean Energy and Technology (CET), Kuala Lumpur, Malaysia, 27–29 June 2011; pp. 51–56.
3. Dos Santos, E.C.; Farias, A.M.; Cavalcanti, M.C.; Bradaschia, F. Integrated three-phase transformerless PV inverter. In Proceedings of the 2012 IEEE International Symposium on Industrial Electronics (ISIE), Hangzhou, China, 28–31 May 2012; pp. 1780–1784.
4. Mehrasa, M.; Pouresmaeil, E.; Pournazarian, B.; Sepehr, A.; Marzband, M.; Catalão, J. Synchronous Resonant Control Technique to Address Power Grid Instability Problems Due to High Renewables Penetration. *Energies* **2018**, *11*, 2469. [[CrossRef](#)]
5. Mehrasa, M.; Pouresmaeil, E.; Taheri, S.; Vechiu, I.; Catalão, J.P. Novel control strategy for modular multilevel converters based on differential flatness theory. *IEEE J. Emerg. Sel. Top. Power Electr.* **2018**, *6*, 888–897. [[CrossRef](#)]
6. Mehrasa, M.; Pouresmaeil, E.; Akorede, M.F.; Zabihi, S.; Catalão, J.P. Function-based modulation control for modular multilevel converters under varying loading and parameters conditions. *IET Gener. Transm. Distrib.* **2017**, *11*, 3222–3230. [[CrossRef](#)]
7. Mehrasa, M.; Pouresmaeil, E.; Zabihi, S.; Vechiu, I.; Catalao, J.P. A multi-loop control technique for the stable operation of modular multilevel converters in HVDC transmission systems. *Int. J. Electr. Power Energy Syst.* **2018**, *96*, 194–207. [[CrossRef](#)]
8. Pouresmaeil, E.; Mehrasa, M.; Catalão, J.P. Control strategy for the stable operation of multilevel converter topologies in DG technology. In Proceedings of the Power Systems Computation Conference (PSCC), Wroclaw, Poland, 18–22 August 2014; pp. 1–7.
9. Blaabjerg, F.; Teodorescu, R.; Liserre, M.; Timbus, A.V. Overview of control and grid synchronization for distributed power generation systems. *IEEE Trans. Ind. Electr.* **2006**, *53*, 1398–1409. [[CrossRef](#)]
10. Xiao, H.; Xie, S. Leakage current analytical model and application in single-phase transformerless photovoltaic grid-connected inverter. *IEEE Trans. Electromagnetic. Compat.* **2010**, *52*, 902–913. [[CrossRef](#)]
11. Lopez, O.; Freijedo, F.D.; Yedes, A.G.; Fernandez-Comesana, P.; Malvar, J.; Teodorescu, R.; Doval-Gandoy, J. Eliminating ground current in a transformerless photovoltaic application. *IEEE Trans. Energy Convers.* **2010**, *25*, 140–147. [[CrossRef](#)]
12. González, R.; Lopez, J.; Sanchis, P.; Marroyo, L. Transformerless inverter for single-phase photovoltaic systems. *IEEE Trans. Power Electr.* **2007**, *22*, 693–697. [[CrossRef](#)]
13. DIN VDE 0126-1-1. Automatic Disconnection Device between Agenerator and the Public Low-Voltage Grid. Available online: <https://www.vde-verlag.de/standards/0100178/din-vde-v-0126-1-1-vde-v-0126-1-1-2013-08.html> (accessed on 10 September 2018).
14. González, R.; Gubía, E.; López, J.; Marroyo, L. Transformerless single-phase multilevel-based photovoltaic inverter. *IEEE Trans. Ind. Electr.* **2008**, *55*, 2694–2702. [[CrossRef](#)]
15. Rashid, M.H. *Power Electronics Handbook*, 2nd ed.; Academic Press: San Diego, CA, USA, 2007.
16. Zhang, L.; Sun, K.; Xing, Y.; Xing, M. H6 transformerless full-bridge PV grid-tied inverters. *IEEE Trans. Power Electr.* **2014**, *29*, 1229–1238. [[CrossRef](#)]

17. Rizzoli, G.; Mengoni, M.; Zarri, L.; Tani, A.; Serra, G.; Casadei, D. Comparison of single-phase H4, H5, H6 inverters for transformerless photovoltaic applications. In Proceedings of the 2016-42nd Annual Conference of the IEEE Industrial Electronics Society, IECON, Florence, Italy, 23–26 October 2016; pp. 3038–3045.
18. Rouzbehi, K.; Davarifar, M.; Martino, M.; Citro, C.; Luna, A.; Daneshifar, Z.; Rodriguez, P. Comparative efficiency study of single phase photovoltaic grid connected inverters using PLECS®. In Proceedings of the 2015 International Congress on Technology, Communication and Knowledge (ICTCK), Mashhad, Iran, 11–12 November 2015; pp. 536–541.
19. Li, H.; Zeng, Y.; Zheng, T.Q.; Zhang, B. A novel H5-D topology for transformerless photovoltaic grid-connected inverter application. In Proceedings of the 2016 IEEE 8th International Power Electronics and Motion Control Conference (IPEMC-ECCE Asia), Hefei, China, 22–26 May 2016; pp. 731–735.
20. Guo, X.; Jia, X.; Lu, Z.; Guerrero, J.M. Single phase cascaded H5 inverter with leakage current elimination for transformerless photovoltaic system. In Proceedings of the 2016 IEEE Applied Power Electronics Conference and Exposition (APEC), Long Beach, CA, USA, 22–24 March 2016; pp. 398–401.
21. Gotekar, P.S.; Muley, S.P.; Kothari, D.P.; Umre, B.S. Comparison of full bridge bipolar, H5, H6 and HERIC inverter for single phase photovoltaic systems-a review. In Proceedings of the 2015 Annual IEEE India Conference (INDICON), New Delhi, India, 17–20 December 2015; pp. 1–6.
22. Freddy, T.K.S.; Rahim, N.A.; Hew, W.P.; Che, H.S. Modulation techniques to reduce leakage current in three-phase transformerless H7 photovoltaic inverter. *IEEE Trans. Ind. Electr.* **2015**, *62*, 322–331. [[CrossRef](#)]
23. Araújo, S.V.; Zacharias, P.; Mallwitz, R. Highly efficient single-phase transformerless inverters for grid-connected photovoltaic systems. *IEEE Trans. Ind. Electr.* **2010**, *57*, 3118–3128. [[CrossRef](#)]
24. Li, W.; Gu, Y.; Luo, H.; Cui, W.; He, X.; Xia, C. Topology review and derivation methodology of single-phase transformerless photovoltaic inverters for leakage current suppression. *IEEE Trans. Ind. Electron.* **2015**, *62*, 4537–4551. [[CrossRef](#)]
25. Li, H.; Zeng, Y.; Zhang, B.; Zheng, Q.; Hao, R.; Yang, Z. An Improved H5 Topology with Low Common-mode Current for Transformerless PV Grid-connected Inverter. *IEEE Trans. Power Electr.* **2018**. [[CrossRef](#)]
26. Kassem, A.M. MPPT control design and performance improvements of a PV generator powered DC motor-pump system based on artificial neural networks. *Int. J. Electr. Power Energy Syst.* **2012**, *43*, 90–98. [[CrossRef](#)]
27. Asim, M.; Tariq, M.; Mallick, M.A.; Ashraf, I.; Kumari, S.; Bhoi, A.K. *Critical Evaluation of Offline MPPT Techniques of Solar PV for Stand-Alone Applications*; Advances in Smart Grid and Renewable Energy, Lecture Notes in Electrical Engineering 435; Springer Nature Singapore Pte Ltd.: Singapore, 2018. [[CrossRef](#)]
28. Sher, H.A.; Murtaza, A.F.; Addoweeesh, K.E.; Chiaberge, M. An intelligent off-line MPPT technique for PV applications. In Proceedings of the Systems, Process & Control (ICSPC), 2013 IEEE Conference on, Kuala Lumpur, Malaysia, 13–15 December 2013; pp. 316–320.
29. Husain, M.A.; Tariq, A.; Hameed, S.; Arif, M.S.B.; Jain, A. Comparative assessment of maximum power point tracking procedures for photovoltaic systems. *Green Energy Environ.* **2017**, *2*, 5–17. [[CrossRef](#)]
30. Das, P. Maximum power tracking based open circuit voltage method for PV system. *Energy Procedia* **2016**, *90*, 2–13. [[CrossRef](#)]
31. Sahu, T.P.; Dixit, T.V. Modelling and analysis of Perturb & Observe and Incremental Conductance MPPT algorithm for PV array using Ćuk converter. In Proceedings of the 2014 IEEE Students' Conference on Electrical, Electronics and Computer Science (SCEECS), Bhopal, India, 1–2 March 2014; pp. 1–6.
32. Safari, A.; Mekhilef, S. Simulation and hardware implementation of incremental conductance MPPT with direct control method using cuk converter. *IEEE Trans. Ind. Electr.* **2011**, *58*, 1154–1161. [[CrossRef](#)]
33. Faranda, R.; Leva, S.; Maugeri, V. MPPT techniques for PV systems: Energetic and cost comparison. In Proceedings of the 2008 IEEE Power and Energy Society General Meeting-Conversion and Delivery of Electrical Energy in the 21st Century, Pittsburgh, PA, USA, 22–24 July 2008; pp. 1–6.
34. Kottas, T.L.; Boutalis, Y.S.; Karlis, A.D. New maximum power point tracker for PV arrays using fuzzy controller in close cooperation with fuzzy cognitive networks. *IEEE Trans. Energy Convers.* **2006**, *21*, 793–803. [[CrossRef](#)]
35. Anzalchi, A.; Sarwat, A. Artificial neural network based Duty Cycle estimation for maximum Power Point tracking in Photovoltaic systems. In Proceedings of the SoutheastCon 2015, Fort Lauderdale, FL, USA, 9–12 April 2015.

36. Kjaer, S.B.; Pedersen, J.K.; Blaabjerg, F. A review of single-phase grid-connected inverters for photovoltaic modules. *IEEE Trans. Ind. Appl.* **2005**, *41*, 1292–1306. [[CrossRef](#)]
37. Zaid, S.A.; Kassem, A.M. Review, analysis and improving the utilization factor of a PV-grid connected system via HERIC transformerless approach. *Renew. Sustain. Energy Rev.* **2017**, *73*, 1061–1069. [[CrossRef](#)]
38. Xing, S.; Chen, S.; Wei, Z.; Xia, J. *Unifying Electrical Engineering and Electronics Engineering: Proceedings of the 2012 International Conference on Electrical and Electronics Engineering*; Springer Science & Business Media: New York, NY, USA, 2014. [[CrossRef](#)]
39. Teodorescu, R.; Blaabjerg, F. Flexible control of small wind turbines with grid failure detection operating in stand-alone and grid-connected mode. *IEEE Trans. Power Electr.* **2004**, *19*, 1323–1332. [[CrossRef](#)]
40. Zhuang, M.; Atherton, D.P. Automatic tuning of optimum PID controllers. *IEE Proc. D-Control Theory Appl.* **1993**, *140*, 216–224. [[CrossRef](#)]
41. Mao, P.; Zhang, M.; Cui, S.; Zhang, W.; Kwon, B.H. A review of current control strategy for single-phase grid-connected inverters. *Telecommun. Comput. Electr. Control* **2014**, *12*, 563–580.
42. Agirman, I.; Blasko, V. A novel control method of a VSC without AC line voltage sensors. *IEEE Trans. Ind. Appl.* **2003**, *39*, 519–524. [[CrossRef](#)]
43. Teodorescu, R.; Blaabjerg, F.; Liserre, M.; Loh, C. Proportional-resonant controllers and filters for grid-connected voltage-source converters. *IEE Proc.-Electr. Power Appl.* **2006**, *153*, 750–762. [[CrossRef](#)]
44. Zhang, N.; Tang, H.; Yao, C. A Systematic method for designing a PR controller and active damping of the LCL filter for single-phase grid-connected PV inverters. *Energies* **2014**, *7*, 3934–3954. [[CrossRef](#)]
45. IEEE Std. *Recommended Practices and Requirements for Harmonic Control in Electrical Power Systems*; IEEE: Piscataway, NJ, USA, 1993; pp. 1–112. [[CrossRef](#)]



© 2018 by the authors. Licensee MDPI, Basel, Switzerland. This article is an open access article distributed under the terms and conditions of the Creative Commons Attribution (CC BY) license (<http://creativecommons.org/licenses/by/4.0/>).